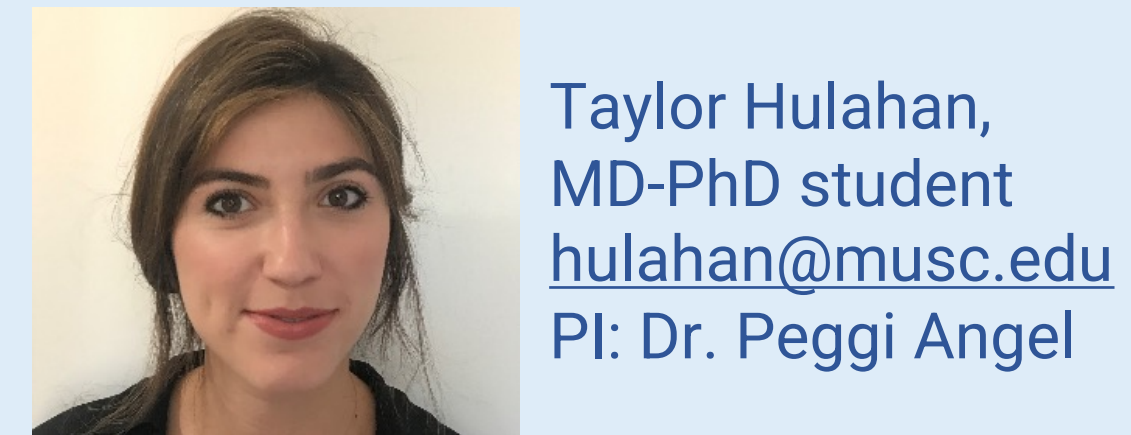


# From the Non-invasive Breast Microenvironment to Metastatic Breast Cancer: Pathological Variation in Collagen Proteomic Signatures by Mass Spectrometry Tissue Imaging

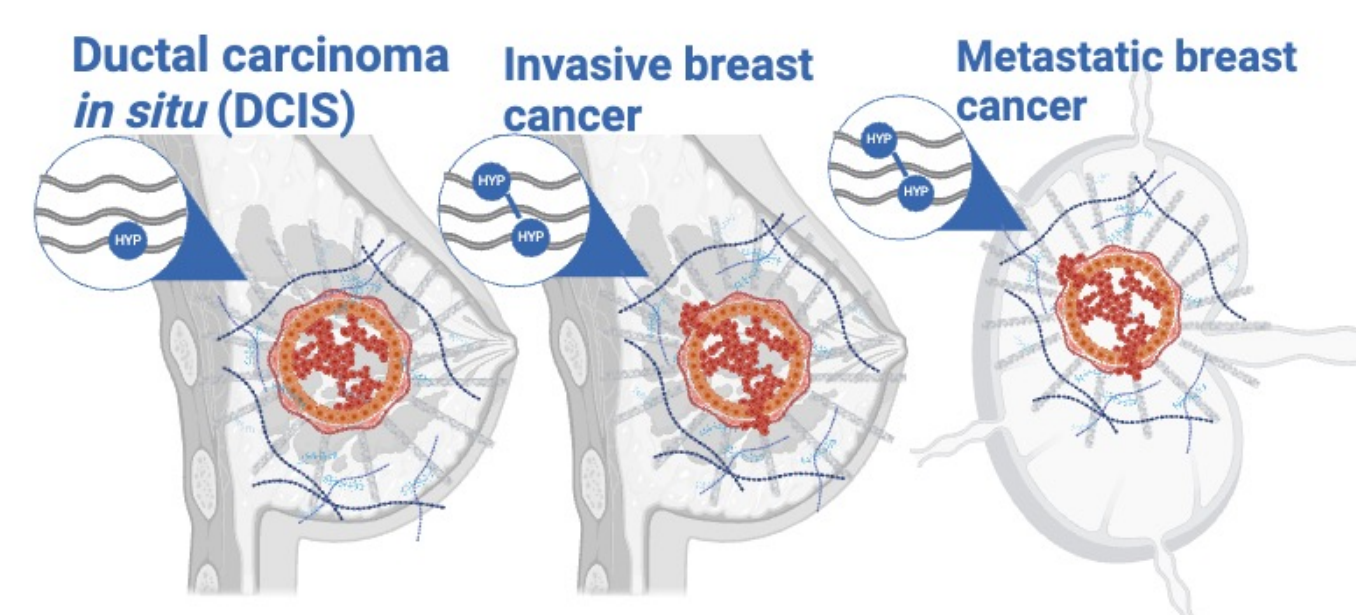
Authors & Affiliations: Taylor S. Hulahan<sup>1</sup>, Ashlyn Ivey<sup>1</sup>, Elizabeth N. Wallace<sup>1</sup>, Laura Spruill<sup>1</sup>, Yeonhee Park<sup>2</sup>, Anand Mehta<sup>1</sup>, Robert West<sup>3</sup>, Robert Michael Angelo<sup>3</sup>, Graham Colditz<sup>4</sup>, Jeffrey R Marks<sup>5</sup>, E Shelley Hwang<sup>5</sup>, Richard R. Drake<sup>1</sup>, Harikrishna Nakshatri<sup>6</sup>, Marvella Ford<sup>1</sup>, Peggi M. Angel<sup>1</sup>

<sup>1</sup>Medical University of South Carolina, <sup>2</sup>University of Wisconsin-Madison, <sup>3</sup>Stanford University, <sup>4</sup>Washington University, <sup>5</sup>Duke University, <sup>6</sup>Indiana University School of Medicine



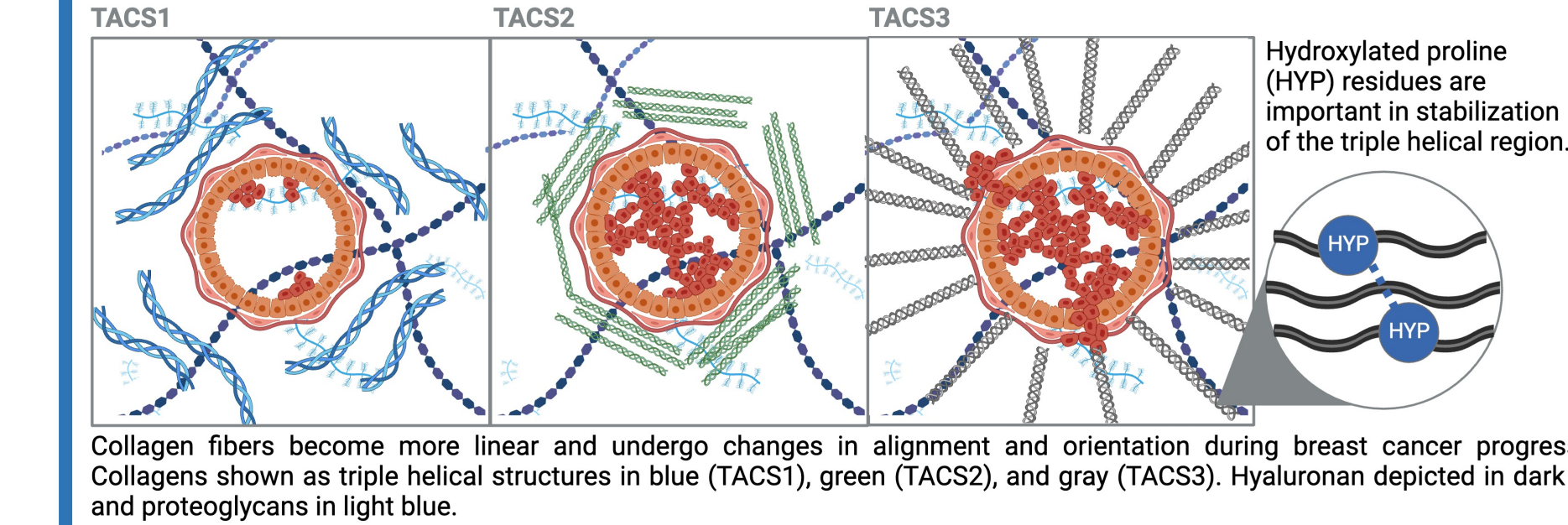
## OVERVIEW

**Overview.** This study represents a comparative investigation of the extracellular matrix (ECM) microenvironment of ductal carcinoma *in situ* (DCIS), invasive breast cancer (IBC), and metastatic breast cancer. Fifty-three specimens and 3 tissue microarrays from 59 breast cancer patients underwent ECM-targeted mass spectrometry imaging. Over 1,000 ECM peptide peaks were detected with many spatially mapping to pathologically annotated regions. Here, we discover intra-tumoral heterogeneity within the local ECM microenvironment surrounding individual DCIS lesions, a distinct proteomic signature between DCIS and invasive ductal carcinoma (IDC) pathologies, and similarities between the primary and secondary tumor sites.



## INTRODUCTION

### Tumor-Associated Collagen Signatures (TACS)

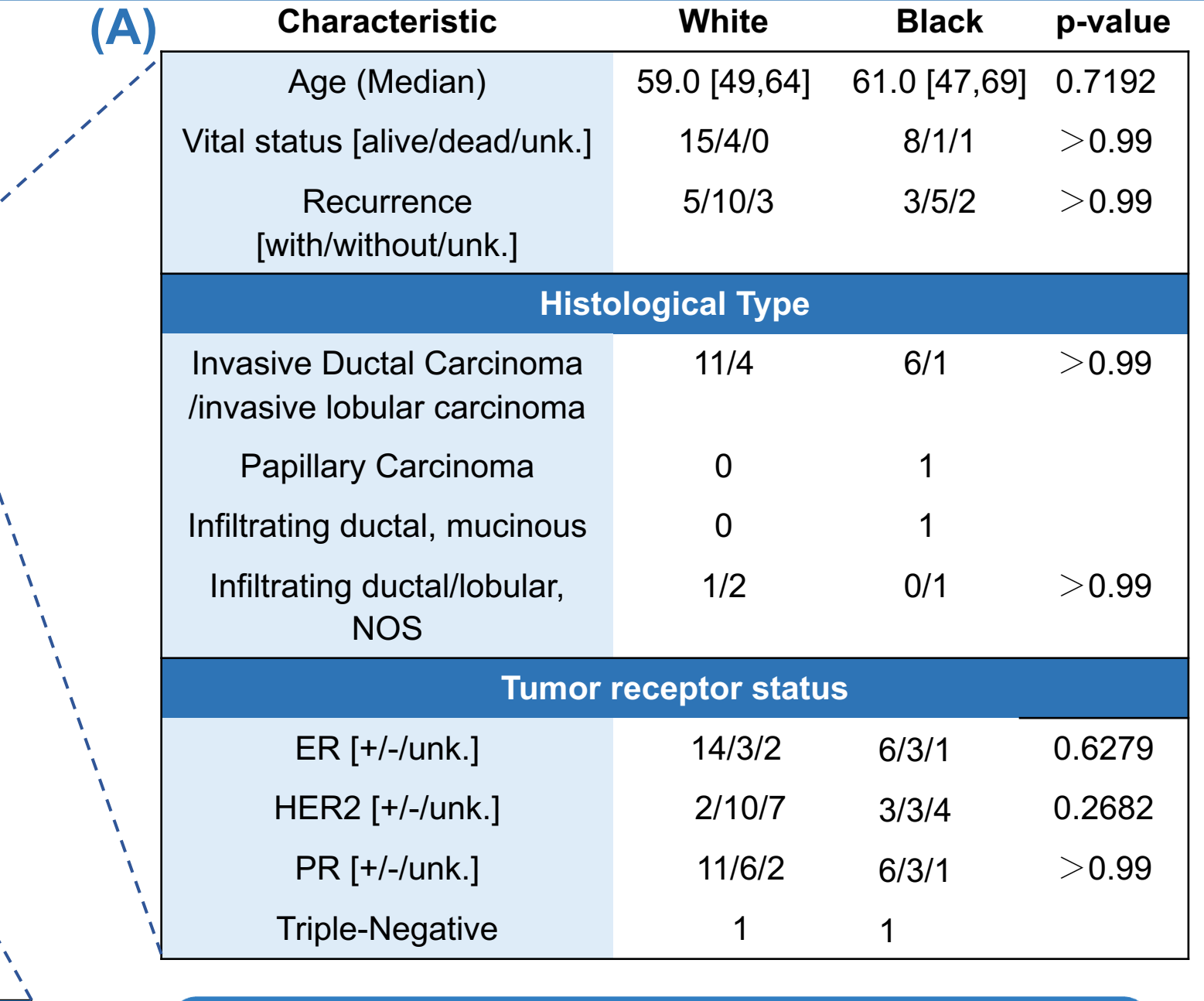


**Introduction.** DCIS represents approximately 20% of breast cancer diagnoses<sup>1</sup>. Although not considered lethal, DCIS patients experience a four times higher breast cancer-specific mortality rate than the general population due to an unpredictable progression to IBC<sup>2</sup>. Subsequent spread to regional areas such as the axillary lymph nodes further decreases survival by 13%<sup>3</sup>. As breast cancer becomes invasive, the collagen-containing basement membrane is disrupted. Collagen also increases in abundance (TACS1), and its fiber alignment changes (TACS2-3)<sup>4,5</sup>. Post-translationally, dysregulation of hydroxylation of prolines (HYP) is hypothesized as prolyl hydroxylases responsible for this modification have been found to be crucial in invasion and metastases<sup>6,7</sup>.

## COHORT CHARACTERISTICS & METHODS

	DCIS	IDC
<b>Pathology</b>		
DCIS only	7 (38.9%)	
Mixed DCIS-IDC	6 (33.3%)	
IDC	4 (22.2%)	
Inflammatory foci	1 (5.6%)	
<b>Nuclear Grade</b>		
1	0 (0%)	0 (0%)
2	3 (23.1%)	2 (20%)
3	10 (76.9%)	8 (80%)
<b>Architecture</b>		
Solid	11 (84.6%)	
Cribriform	3 (23.1%)	
Comedo Necrosis	6 (46.2%)	
Micropapillary	1 (7.7%)	
<b>Surgical Treatment</b>	n=11	
Lumpectomy	5 (45.5%)	
Partial mastectomy	3 (27.3%)	
Mastectomy	4 (27.3%)	
<b>Race</b>	n=6	
African American	1 (16.7%)	
White	5 (83.3%)	

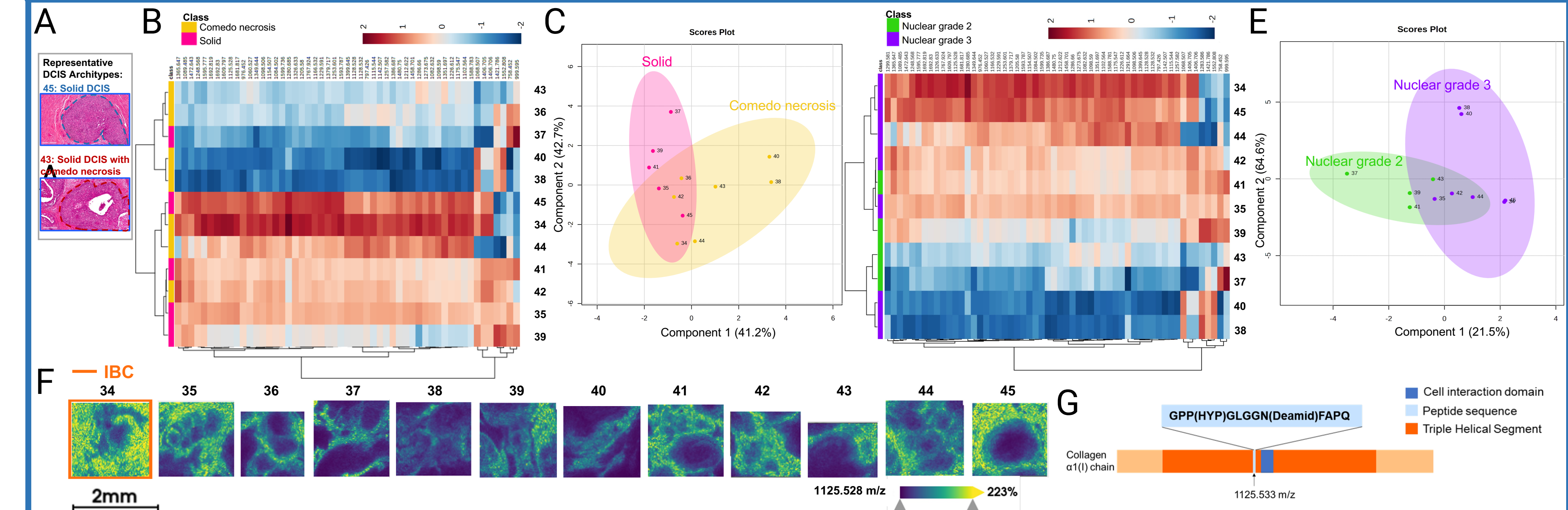
	White	Black	p-value
Age (Median)	59.0 [49,64]	61.0 [47,69]	0.7192
Vital status [alive/dead/unk.]	15/4/0	8/1/1	> 0.99
Recurrence [with/without/unk.]	5/10/3	3/5/2	> 0.99
<b>Histological Type</b>			
Invasive Ductal Carcinoma /invasive lobular carcinoma	11/4	6/1	> 0.99
Papillary Carcinoma	0	1	
Infiltrating ductal, mucinous	0	1	
Infiltrating ductal/lobular, NOS	1/2	0/1	> 0.99
<b>Tumor receptor status</b>			
ER [+/-/unk.]	14/3/2	6/3/1	0.6279
HER2 [+/-/unk.]	2/10/7	3/3/4	0.2682
PR [+/-/unk.]	11/6/2	6/3/1	> 0.99
Triple-Negative	1	1	



**Methods.** Samples were annotated as DCIS, mixed DCIS-IBC, IBC, benign lymph nodes, or metastatic lymph nodes. Samples were digested with PNGase F and deglycosylated to increase COLase III access. Following COLase III digest, MALDI-QTOF imaging was performed, capturing various collagen types and approximately 40 other ECM proteins associated with collagen. Liquid chromatography tandem mass spectrometry (LC-MS/MS) was used for peptide identification.

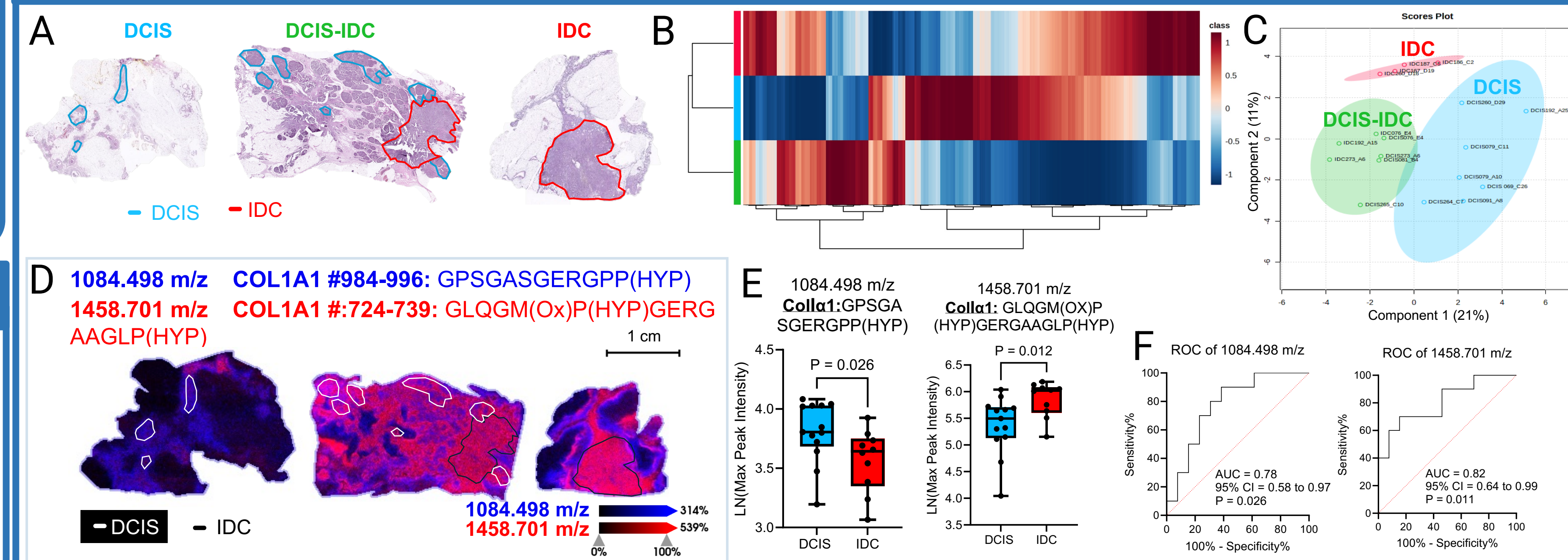
Characteristic	Number (%)
<b>Race</b>	
White	3 (27.27%)
Black	7 (63.63%)
Asian	1 (9.09%)
<b>Median Age of Dx</b>	63 years old
<b>BMI</b>	
18.5-24.9	1 (9.09%)
25.0-29.9	4 (36.36%)
<30	6 (54.45%)
<b>Menopausal status</b>	
Pre-menopausal	0 (0%)
Post-menopausal	11 (100%)

## RESULT A: Intra-tumoral Heterogeneity Reported in the DCIS ECM Microenvironment



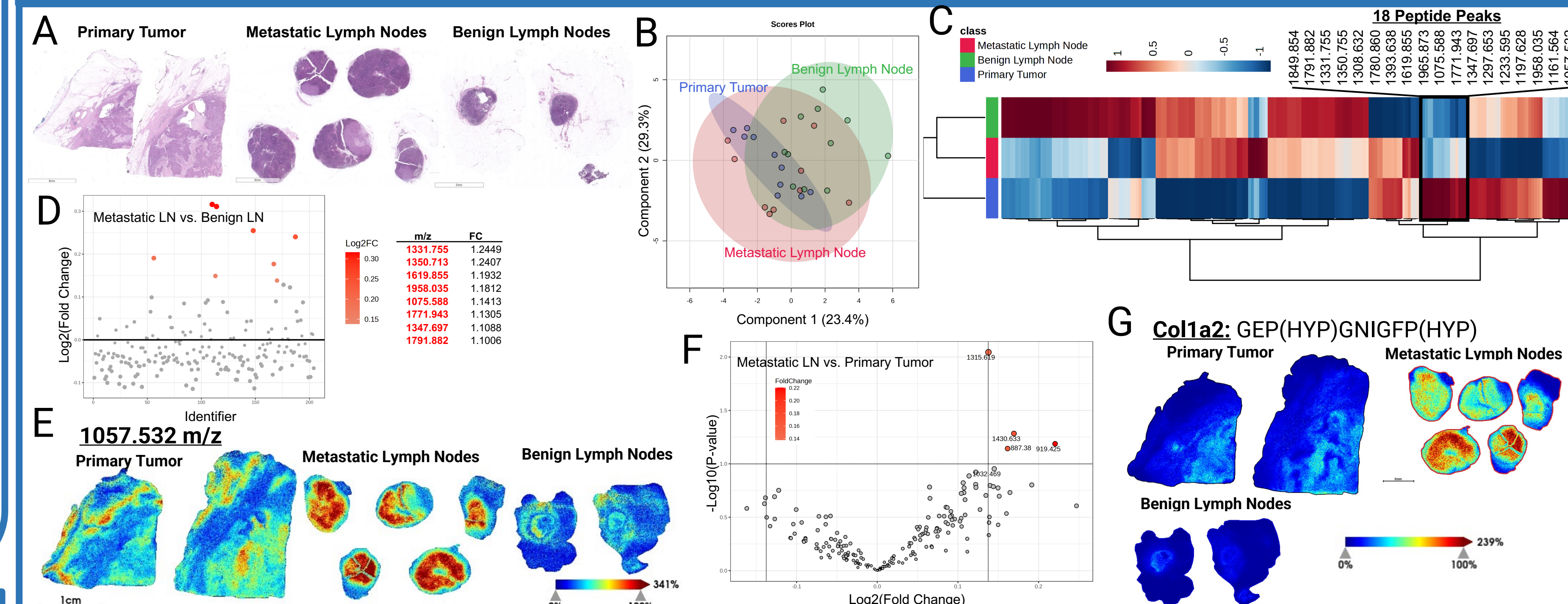
**Result A: Intra-tumoral Heterogeneity Reported in the DCIS ECM Microenvironment.** (A) Representative H&E images of individual lesions from a mixed DCIS-IBC specimen. Heat map of 56 ECM peptide intensities stratified by architectural pattern (B) and nuclear grade (D). Partial squares least discriminant analysis by architectural pattern (C) and by nuclear grade (E). (F-G) Spatial MSI images from each ROI with peptide identification. Peptide mapped to COL1A1 near its reported cell interaction domain.

## RESULT B: Differential Expression of HYP Collagen Sequences between DCIS & IDC Regions



**Result B: Differential Expression of HYP Collagen Sequences between DCIS & IDC Regions.** (A) Three representative H&E images each pathology classification are depicted. Pathologist's annotations use red to denote IDC lesions and blue to define DCIS lesions. (B) Heat map of 1,005 putatively identified peptides were differentially expressed between IDC and DCIS regions in the specimens (n=17; p<0.01 by unpaired two-tailed t-test). Note: one lumpectomy sample was excluded as it was determined to not have DCIS or IDC present. (C) Sparse Partial Least Squares Discriminant Analysis shows distinct clustering of DCIS (in blue), DCIS-IDC (in green), and IDC lumpectomies (in blue). (D) Spatial heat maps of MALDI-QTOF imaging of 1084.498 m/z and 1458.701 m/z from three lumpectomies. (E) Two collagen peptides with hydroxylated proline (HYP) residues that have differential intensities between DCIS (n=14) than IDC (n=10) lesions by unpaired two-tailed t-test (p<0.05). OX denotes oxidation. (F) ROC analysis of peaks 1084.498 m/z and 1458.701 m/z (AUROC>0.75 and p<0.05 by Wilson/Brown t-test) are shown. PPM calculations between MALDI-QTOF imaging and LC-MS/MS were within 5 mass accuracy.

## RESULT C: Lymph Node Metastases Exhibit ECM Proteomic Similarities to the Primary Tumor



**Result C. Lymph Node Metastases Exhibit ECM Proteomic Similarities to the Primary Tumor.** (A) Representative hematoxylin and eosin-stained sections are shown. (B) Sparse partial least squares discriminant analysis of 205 putatively identified peaks demonstrates overlapping clustering of benign lymph nodes (n=10), lymph node metastases (n=10), and primary tumor specimens (n=11). (C) Heat map of 205 putatively identified peptide peaks with average intensity profiles between specimen sites. (D) Plot of fold changes reporting in red peptide peaks with increased intensities in metastatic lymph nodes compared to benign lymph node specimens. (E) Spatial heat map of 1057.532 m/z (a currently unidentified peptide) with high peak intensity denoted in red from one patient. (F) Volcano plot demonstrates peptides with increased intensities (shown in red) in the lymph node metastases compared to the primary tumor (p<0.1, FC>1.1). (G) Spatial heat map of 919.425 m/z with high peptide peak intensity denoted in red from one patient.

## CONCLUSIONS & FUTURE DIRECTIONS

- Variation of the ECM proteome between DCIS lesions reveals intra-tumoral heterogeneity within the ECM microenvironment.
- ECM profiles are unique based on pathological classification as DCIS, DCIS-IDC, and IDC and could have predictive value in identifying DCIS patients at increased recurrence risk.
- In metastasis, the axillary lymph node reports proteomic similarities to the primary tumor site.
- Future work will define stromal differences with recurrence in the Resource of Archival Human Breast Cancer Tissue cohort.

## ACKNOWLEDGEMENTS

MUSC Angel Lab, MUSC Drake Lab, our collaborators, and the patients who made this study possible. **Funding:** NIH/NCI R01CA253460; 5T32 GM008716-24; 5T11TR001451-09

### REFERENCES:

1. J. Feinberg et al. *Cancer Treatment and Research* (2018)
2. G. S. Mannu et al. *BMJ* (2024)
3. SEER Database (2013-2019).
4. E. A. Brett et al. *Cancer & Metabolism* (2020)
5. M. W. Conklin et al. *The American Journal of Pathology* (2011)
6. M. Nokelainen et al. *Eur J Biochemistry* (2001).
7. G. Xiong et al. *BMC Cancer* (2014)